

Learning from Mistakes: Post-Training for Driving VLA with Takeover Data

Yinfeng Gao^{1,2,3} [†], Deqing Liu³ [†], Qichao Zhang³ [✉], Yupeng Zheng³, Haochen Tian^{2,3}, Guang Li², Hangjun Ye², Long Chen² [‡], Da-Wei Ding¹ [✉], and Dongbin Zhao³

¹ University of Science and Technology Beijing

² Xiaomi EV

³ Institute of Automation, Chinese Academy of Sciences

[†] Equal contribution. [‡] Project Leader. [✉] Corresponding author.

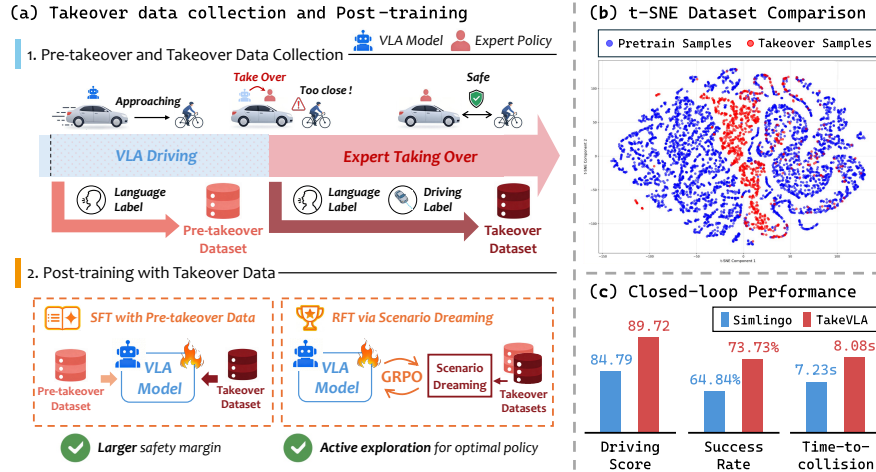


Fig. 1: We propose **TakeVLA**, a post-training framework for driving VLA with takeover data. (a) TakeVLA iteratively collects takeover data via online expert interventions and conducts post-training on the collected data. It introduces *pre-takeover* supervision for larger safety margins and *Scenario Dreaming* for active exploration toward optimal policy. (b) t-SNE visualization shows that the takeover dataset (red) provides valuable OOD samples compared to the pretrain dataset (blue). (c) Closed-loop evaluation on Bench2Drive demonstrates TakeVLA’s superior performance, with a higher driving score, success rate, and significantly improved safety margins.

Abstract. Current Vision-Language-Action (VLA) paradigms in end-to-end autonomous driving rely on offline training from static datasets,

Work done while Yinfeng Gao interns at Xiaomi Embodied Intelligence Team.

leaving them vulnerable to distribution shift. Recent post-training methods use takeover data to mitigate this by augmenting the dataset with high-quality expert takeover samples, yet they suffer from two key limitations: supervision restricted to the period after the takeover moments leads to policies with limited safety margins, and passive preference optimization lacks active exploration for optimal performance. In this paper, we propose **TakeVLA**, a novel VLA post-training framework that overcomes these shortcomings through two complementary innovations. First, we introduce pre-takeover language supervision, which allows the VLA to learn from mistakes proactively. By explicitly teaching the model about what to do in error-prone situations, we cultivate a precautionary mindset that anticipates hazards early and substantially enlarges safety margins. Second, we propose Scenario Dreaming, a reinforcement fine-tuning paradigm that operates in reconstructed takeover scenarios, encouraging active exploration beyond mere preference fitting. Experiments on the Bench2Drive benchmark demonstrate that TakeVLA achieves state-of-the-art closed-loop performance, surpassing the strong VLA baseline SimLingo by 4.93 in driving score, with an enhanced safety margin as evidenced by an 11.76% increase in average TTC.

Keywords: End-to-end Autonomous Driving · Vision-Language-Action Model · Takeover Data · Reinforcement Learning

1 Introduction

Vision-Language-Action (VLA) models have emerged as a promising paradigm for end-to-end autonomous driving [4]. By aligning vision, language, and action spaces, VLAs offer more interpretable and generalizable decision-making than traditional modular pipelines or pure vision-action approaches [20, 49].

Despite these advantages, most VLA-based driving methods are trained on large-scale offline datasets via imitation learning (IL) [13, 38, 54] or reinforcement learning (RL) [24, 34, 46], making them inherently vulnerable to distribution shift due to the lack of safety-critical or out-of-distribution (OOD) samples [42]. Online RL-based methods attempt to address this through trial-and-error exploration in the environment [12, 14, 48], but this often leads to high safety risks and computational costs, as agents frequently enter dangerous or irrelevant regions. Recently, post-training approaches leveraging expert takeover data have gained attention [2, 10, 27]. These methods integrate expert interventions into the training loop: when the policy exhibits unsafe or suboptimal behavior, an expert driver takes over, providing high-quality corrective samples at low trial-and-error cost and effectively augmenting the dataset with valuable safety-critical and OOD demonstrations. However, prior methods with takeover data suffer from two fundamental limitations. First, supervision signals are restricted to the period after the takeover moments, yielding policies with insufficient safety margins. Second, reliance on passive preference learning (*e.g.*, DPO-style optimization [31]) lacks active exploration, resulting in static fitting to demonstrated actions, which limits further performance gains.

We propose **TakeVLA**, a novel VLA post-training framework that addresses these gaps through two key innovations, as illustrated in Fig. 1. First, to mitigate the limited safety margin issue in prior methods, we introduce **pre-takeover** supervision. For each takeover segment, we extend labeling backward from the takeover moment to cover a preceding time window. Since the expert has not yet intervened and no driving action supervision is available, we generate language supervision based on the specific takeover cause. Supervised fine-tuning (SFT) on pre-takeover samples enables the model to anticipate hazards earlier through refined language outputs. By leveraging the VLA model’s inherent ability to align linguistic semantics with low-level actions [37], the resulting language-conditioned actions substantially enlarge safety margins in error-prone situations. Second, to overcome the lack of active exploration in preference-based optimization, we introduce a novel task termed **Scenario Dreaming**. By reconstructing takeover scenarios in a pseudo-simulation environment, we apply reinforcement fine-tuning (RFT) to encourage the exploration of superior language outputs, leading to more effective driving actions in safety-critical situations and going beyond mere fitting of expert preferences.

We train and evaluate TakeVLA on the challenging Bench2Drive [17] closed-loop benchmark. Experimental results show consistent gains from both pre-takeover supervision and Scenario Dreaming. TakeVLA achieves a driving score of 89.72, representing a substantial improvement of 4.93 over the strong VLA baseline SimLingo [32]. Notably, without any rule-based post-processing, TakeVLA outperforms SimLingo by 7.25. Furthermore, pre-takeover training significantly enlarges safety margins, with average Time-to-Collision (TTC) increased by 11.76% over SimLingo, validating the effectiveness of our designs.

Our main contributions are summarized as follows:

- We propose **TakeVLA**, a novel post-training framework for VLA-based autonomous driving. To our knowledge, it is the first method that exploits the inherent language-action alignment ability of VLAs to learn from pre-takeover contexts, enabling precautionary decision-making in language space and safe navigation in error-prone scenarios.
- We introduce Scenario Dreaming, a novel reinforcement fine-tuning task that leverages reconstructed takeover scenarios for active exploration toward optimal policies, substantially enhancing performance in safety-critical scenarios.
- Experiments on the Bench2Drive benchmark demonstrate that TakeVLA achieves state-of-the-art closed-loop performance, surpassing SimLingo by 4.93 in driving score, while substantially improving safety margins, yielding an 11.76% increase in average TTC.

2 Related Works

2.1 End-to-end Autonomous Driving

End-to-end autonomous driving has seen rapid progress in recent years. Foundational works [16, 19] established the paradigm of a holistic Transformer that

maps raw sensor inputs directly to low-level driving actions, often augmented with auxiliary supervision for perception and prediction. Subsequent efforts have explored more efficient architectures [39, 51], multi-modal planning [5, 26, 43], and self-supervised training [23, 53] to improve scalability and performance. However, these vision-only approaches lack rich world knowledge and explicit reasoning, resulting in limited interpretability and degraded performance in complex scenarios. VLA models [1, 21] address this limitation by integrating pre-trained vision-language models to inject commonsense knowledge and semantic reasoning capabilities [52]. LMDrive [35] pioneered language-guided closed-loop driving using natural-language instructions. ORION [11] introduced a generative trajectory decoder for more feasible actions. SimLingo [32] and Alpamayo-R1 [44] aligned reasoning with actions through counterfactual language-action pairs and alignment-reward-based RL, respectively. AutoVLA [54] further enabled adaptive chain-of-thought reasoning conditioned on scene complexity via RL fine-tuning. Nevertheless, these VLA methods rely exclusively on offline static datasets, leaving them vulnerable to distribution shift and poor recovery in unexpected situations.

2.2 Post-training with Takeover Data

Recent approaches leverage online expert interventions to collect high-quality takeover samples from safety-critical or unexpected situations without incurring real accidents, enabling low-risk policy improvement beyond static offline datasets. PPL [2] converts takeovers into predictive preference labels over future trajectories and applies contrastive preference optimization to boost policy performance. TakeAD [27] extends preference-based post-training to end-to-end policies through iterative refinement with takeover data, achieving significant gains in closed-loop performance. CoReVLA [10] applies a similar preference-based optimization to VLA models to handle long-tail scenarios. Despite these advances, existing methods share two key limitations: supervision restricted to the period after takeover moments yields policies with limited safety margins, while reliance on passive preference-based optimization lacks active exploration, resulting in static fitting to demonstrated actions. Building on recent findings that language can effectively steer and refine low-level actions [37], TakeVLA overcomes these limitations by performing pre-takeover supervision in the language space to enlarge safety margins, and by introducing Scenario Dreaming to enable active exploration for RL in reconstructed takeover scenarios.

2.3 Reinforcement Fine-tuning for End-to-end Driving

Reinforcement fine-tuning (RFT) enables pre-trained policies to discover optimal behaviors through active exploration [29, 30, 50]. Existing RFT methods for end-to-end autonomous driving fall into two main categories. Offline approaches [24, 46, 54] train solely on static datasets and suffer from distribution shift due to the absence of real environment interactions. Online methods [12, 48] rely on large-scale trial-and-error in real environments, incurring high safety

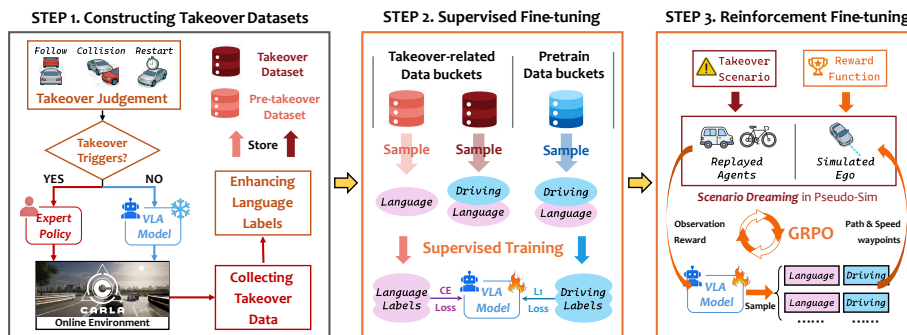


Fig. 2: Post-training pipeline for TakeVLA. Starting from a pre-trained VLA model, each round consists of three key steps: (1) online interaction with expert takeovers to construct pre-takeover and takeover datasets, (2) supervised fine-tuning on the constructed datasets, and (3) reinforcement fine-tuning via Scenario Dreaming in reconstructed takeover scenarios. Multiple rounds progressively enhance language-conditioned driving performance.

risks and computational costs from exploring dangerous or irrelevant states. In this work, we construct offline RL training scenarios from online-collected expert takeover data. These takeovers naturally constrain exploration costs by preventing actual accidents, while providing scene information to reconstruct safety-critical takeover scenarios for safe trial-and-error during reinforcement fine-tuning.

3 Problem Formulation

We formulate VLA-based end-to-end autonomous driving as a Partially Observable Markov Decision Process (POMDP) [40], defined by the tuple $(\mathcal{O}, \mathcal{S}, \mathcal{A}, P, O, r, \gamma)$. Here, \mathcal{O} , \mathcal{S} , and \mathcal{A} denote the observation, state, and action spaces, respectively. P and O are the state transition and observation functions, r is the reward function, and $\gamma \in [0, 1)$ is the discount factor. Concretely, the observation space is $\mathcal{O} = \{o_l, o_v\}$, comprising natural language instructions o_l and visual inputs o_v . The state space \mathcal{S} represents the unobservable ground-truth environmental state. The action space is $\mathcal{A} = \{a_l, a_d\}$, where a_l is the generated language output consisting of a meta-action and an accompanying reason, and a_d denotes the physical driving action.

The learned VLA policy is parameterized as $\pi(a_l, a_d | o_l, o_v)$. In practice, expert takeover policies are typically human-provided. To ensure behavioral consistency, optimality, and scalability, we adopt the privileged rule-based *PDM-Lite* [38, 55] expert policy $\hat{\pi}(a_d | s)$, $s \in \mathcal{S}$, which generates expert driving actions \hat{a}_d using full simulator ground-truth information. During online interaction, the predicted driving actions a_d are converted via a low-level PID controller into throttle, brake, and steering commands applied to the ego-vehicle.

4 Method

We propose **TakeVLA**, a post-training framework to enhance pre-trained VLA models for end-to-end autonomous driving. As illustrated in Fig. 2, TakeVLA starts from a pre-trained VLA and iteratively performs multiple rounds of takeover datasets construction and post-training to progressively improve performance. Each round comprises three key steps: (1) online interaction with expert takeovers to construct pre-takeover and takeover datasets, (2) supervised fine-tuning on the constructed datasets, and (3) reinforcement fine-tuning via Scenario Dreaming in reconstructed takeover scenarios.

4.1 VLA Model Architecture and Pre-training

We adopt SimLingo [32] as our baseline VLA model, which employs a Chain-of-Thought approach by conditioning driving actions on generated language. As illustrated in Fig. 3, the model takes a front-view camera image o_v (448×896) and a language instruction o_l (including vehicle speed and task prompts) as inputs. o_v is encoded into visual features F_v via InternViT [6], while o_l is tokenized into language embeddings F_l . These features are fed into the LLM (Qwen2-0.5B [45]) to autoregressively generate the language action a_l . SimLingo decouples the driving action a_d into path and speed waypoints, representing spatially and temporally equidistant coordinate sequences. Specifically, two learnable queries q_d^{path} and q_d^{spd} aggregate information from F_l , F_v , and a_l in a single forward pass through the LLM. The resulting query features are then passed to a Multi-Layer Perceptron decoder to produce the final coordinate sequences.

For simplicity, we omit the encoding of future navigation information in the figure and description. But note that they are also part of LLM’s inputs, provided as additional language prompts or target point embeddings.

Pre-training Process. Following SimLingo [32], we perform supervised pre-training on data collected by the privileged *PDM-Lite* [38, 55] expert. The pre-training dataset $\mathcal{D}_{pretrain}$ contains approximately 3.1 million driving frames at 4 fps. Pre-training uses the default configuration: bucket sampling for mitigating imbalanced data distribution, VQA tasks for vision-language understanding, and action dreaming tasks for robust language-action alignment.

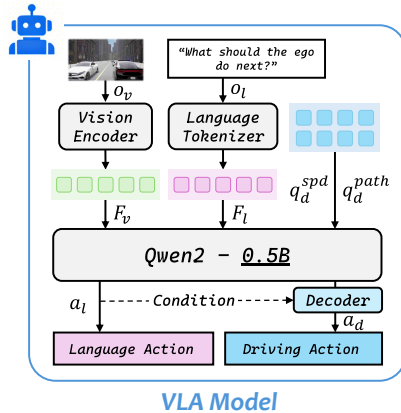


Fig. 3: Architecture of the baseline VLA model.

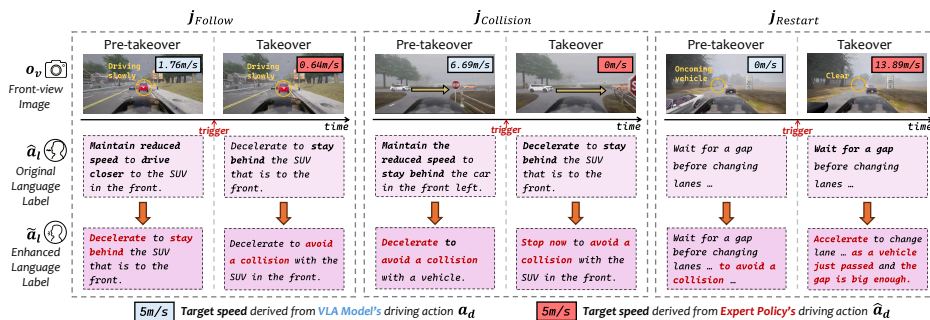


Fig. 4: Language label enhancement. For each takeover trigger type (Follow, Collision, Restart), original language labels (middle) are refined (bottom) based on the specific cause. Enhanced labels emphasize urgency and explicit causality, leading to more conservative and effective driving actions in critical scenarios.

4.2 Constructing Takeover Datasets

Collecting Takeover Data. During online interaction between the VLA policy π and the environment, the expert policy $\hat{\pi}$ runs in shadow mode to monitor and be ready to intervene [27]. We define takeover judgment conditions $J = \{j_{Follow}, j_{Collision}, j_{Restart}\}$ to trigger takeover. Specifically, j_{Follow} is triggered in car-following scenarios when the expert indicates deceleration, but the VLA fails to respond for 0.5 seconds, $j_{Collision}$ activates when a collision is predicted within 1 second under constant velocity, and $j_{Restart}$ engages when the ego-vehicle is stuck in high-density traffic due to missing lane-change opportunities. Any triggered condition signals policy failure and prompts immediate expert takeover for T_{take} frames. By default, T_{take} is set to 50 frames, corresponding to 2.5 seconds at 20 fps in the interaction environment. For each triggered takeover at time t , we collect the raw takeover data sequence $\{o_l, o_v, \hat{a}_l, \hat{a}_d\}_t^{t+T_{take}}$, where \hat{a}_d is the expert driving action, and \hat{a}_l is the language label derived from the expert’s internal logic.

Enhancing Language Labels for Takeover Data. The original language label \hat{a}_l from the expert’s internal logic may lack sufficient urgency or explicit causality, limiting the model’s ability to learn timely avoidance in takeover scenarios. To address this, we enhance \hat{a}_l based on the specific trigger $j \in J$ to produce the refined label \tilde{a}_l . For example, when $j_{Collision}$ triggers emergency braking, the original label “Decelerate to stay behind ...” becomes “Stop now to avoid a collision ...”. Fig. 4 illustrates further examples. The enhanced label \tilde{a}_l forms the final takeover data sequence $\{o_l, o_v, \tilde{a}_l, \hat{a}_d\}_t^{t+T_{take}}$.

Pre-Takeover Data Construction. To improve language output quality prior to the takeover moments and substantially enlarge safety margins, we additionally collect pre-takeover data. Since no expert intervention occurs in this phase, no ground-truth expert driving actions are available. Thus, pre-takeover data sequence is represented as $\{o_l, o_v, \tilde{a}_l\}_{t-T_{pre}}^{t-1}$, where T_{pre} is the pre-takeover horizon. The language labels \tilde{a}_l are generated using the language label enhance-

ment strategy described earlier based on the impending takeover reason $j \in J$, yielding proactive warning-style output that enables earlier hazard detection. By default, we set the pre-takeover horizon $T_{pre} = 20$ frames, corresponding to 1 second at 20 fps in the online environment.

The resulting takeover and pre-takeover data sequences are stored in the corresponding datasets $\mathcal{D}_{takeover}$ and $\mathcal{D}_{pre-takeover}$ for subsequent post-training.

4.3 Supervised Fine-tuning with Pre-takeover Data

Using the takeover dataset $\mathcal{D}_{takeover}$ and pre-takeover dataset $\mathcal{D}_{pre-takeover}$, we first apply supervised fine-tuning (SFT) to the VLA model to simultaneously improve the quality of its language output and corresponding driving actions in takeover scenarios. To mitigate catastrophic forgetting, we adopt a DAgger-style [33] sampling strategy that mixes samples from the original pretraining dataset $\mathcal{D}_{pretrain}$ and the takeover datasets. As described in Sec. 4.1, the VLA model’s supervised training employs bucket sampling. During SFT, we sample with a probability of p from buckets built from $\mathcal{D}_{takeover}$ and $\mathcal{D}_{pre-takeover}$, and with a probability of $1-p$ from the original buckets of $\mathcal{D}_{pretrain}$. By default, p is set to 0.2 to prioritize takeover samples while preserving pre-training knowledge.

The sampled batches are supervised using cross-entropy loss on the language output a_l against the enhanced language label \tilde{a}_l and smooth-L1 loss on the predicted driving action a_d against the expert driving action \hat{a}_d . For pre-takeover samples that lack actual expert driving actions, we apply a mask that disables driving action supervision while retaining language supervision. For a sampled instance i , the SFT loss is formulated as:

$$\mathcal{L}_i^{\text{SFT}} = \mathcal{L}_i^{\text{Cross-Entropy}}(a_l, \tilde{a}_l) + (1 - m_i)\mathcal{L}_i^{\text{Smooth-L1}}(a_d, \hat{a}_d), \quad (1)$$

where $m_i = 1$ for pre-takeover samples and $m_i = 0$ for takeover and pre-training samples. Throughout the SFT process, we maintain the Action Dreaming task to preserve the VLA model’s language-action alignment capability.

4.4 Reinforcement Fine-tuning via Scenario Dreaming

Following SFT, we employ reinforcement fine-tuning (RFT) to further optimize the VLA model for takeover scenarios. Since all RL training occurs in reconstructed scenes derived from samples of $\mathcal{D}_{takeover}$ and $\mathcal{D}_{pre-takeover}$, rather than real-world execution, we refer to this process as *Scenario Dreaming*.

The RL exploration is conducted in a vector-space pseudo-simulation environment [3, 8], utilizing ground-truth annotations from the datasets. Specifically, for each sample, we simulate a 2-second future driving scene at 5 Hz, resulting in a simulation horizon of $H = 10$. Ego-vehicle dynamics are modeled using a bicycle model, with control signals generated by the same PID controller used in online deployment. Other agents’ trajectories are replayed from recorded ground-truth future positions. The reward function is defined as:

$$r_\tau = -r_\tau^{dis} - r_\tau^{col}, \quad R = \sum_{\tau=0}^H \gamma^\tau r_\tau \quad (2)$$

where τ denotes the simulated time step, r_τ^{dis} is the L2 distance between the ego trajectory and the expert takeover trajectory at time τ , and $r_\tau^{col} = 30$ indicates whether the ego vehicle’s bounding box overlaps with another agent’s box at time τ , and 0 otherwise. R is the discounted cumulative reward.

We use Group Relative Policy Optimization [36] (GRPO) for RL. For each takeover sample i , the old policy π_{old} samples a group of candidate actions $\{a_j\}_{j=1}^G$ with a group size G and evaluates the corresponding rewards $\{R_j\}_{j=1}^G$ via pseudo-simulation. The current policy π is then updated using the loss function:

$$\mathcal{L}_i^{RFT} = \mathcal{L}_i^{GRPO} + \lambda \cdot \mathcal{L}_i^{KL}(\pi \parallel \pi_{ref}), \quad \mathcal{L}_i^{GRPO} = -\frac{1}{G} \sum_{j=1}^G A_j \cdot \left(\frac{\pi(a_j | o)}{\pi_{old}(a_j | o)} \right) \quad (3)$$

where $A_j = (R_j - \text{mean}(\{R_k\}_{k=1}^G)) / \text{std}(\{R_k\}_{k=1}^G)$ is the normalized group-relative advantage, and $\mathcal{L}_i^{KL}(\pi \parallel \pi_{ref})$ is the Kullback-Leibler (KL) divergence loss to prevent policy degradation due to excessive exploration, with π_{ref} being the reference policy from the SFT stage and λ being the KL loss weight. We perform a single policy update per step without clipping to simplify the training as in [54].

5 Experiments

5.1 Experimental Setup

Benchmark and Metrics. We train and evaluate TakeVLA on the Bench2Drive (B2D) closed-loop benchmark [17], which is built on the CARLA simulator [9]. We follow the official Bench2Drive (B2D) protocol, which evaluates models on 220 challenging routes spanning 44 interactive scenario types, under diverse weather conditions and across different towns. Multiple metrics are used to assess driving performance. The **Driving Score (DS)** integrates Route Completion and Infraction Score, capturing both task accomplishment and adherence to traffic rules. The **Success Rate (SR)** represents the proportion of routes that are completed within the required time without any violations. **Efficiency** assesses the ego vehicle’s speed relative to surrounding traffic. **Comfortness** measures the smoothness of the driving trajectory.

Takeover Dataset Collection and Usage. The post-training is performed iteratively over 3 rounds. As outlined in Sec. 4, each round consists of takeover datasets construction, SFT, and RFT. Specifically, the latest model is deployed in each round to collect approximately 40k takeover and 10k pre-takeover samples, totaling 50k takeover-related samples per round. To **prevent data leakage**, all data are collected exclusively from the CARLA Leaderboard v2 training routes, which are strictly disjoint from the evaluation routes. During SFT, we implement a bucket sampling strategy [32] with 500k samples per epoch, where samples are drawn from the takeover-related and original pre-training datasets with probabilities p and $1 - p$, respectively. We set $p = 0.2$ by default. RFT further utilizes both pre-takeover and takeover data for Scenario Dreaming.

Table 1: Closed-loop and Multi-ability performance of SoTA methods on the Bench2Drive leaderboard.

Methods	Reference	Closed-loop Metric \uparrow				Multi-ability (%) \uparrow					
		DS	SR (%)	Efficiency	Comfortness	Merging	Overtaking	Emergency Brake	Give Way	Traffic Sign	Mean
<i>End-to-end Methods</i>											
UniAD [16]	CVPR 23	45.81	16.36	129.21	43.58	12.16	20.00	23.64	10.00	13.89	15.89
VAD [19]	ICCV 23	42.35	15.00	157.94	46.01	7.14	20.00	16.36	20.00	20.22	16.75
SparseDrive [39]	ICRA 25	44.54	16.71	170.21	48.63	12.18	23.19	17.91	20.00	20.98	17.45
DriveTrans.-L. [18]	ICLR 25	63.46	35.01	100.64	20.78	17.57	35.00	48.36	40.00	52.10	38.60
DiffusionDrive [26]	CVPR 25	77.68	52.72	248.18	24.56	50.63	26.67	68.33	50.00	76.32	54.38
Hydra-Next [25]	ICCV 25	73.86	50.00	197.76	20.68	40.00	64.44	61.67	50.00	50.00	53.22
TF++ [55]	CVPRW 24	84.21	67.27	-	-	58.75	57.77	83.33	40.00	82.11	64.39
Raw2Drive [48]	NeurIPS 25	71.36	50.24	214.17	22.42	43.35	51.11	60.00	50.00	62.26	53.34
Hip-AD [41]	ICCV 25	86.77	69.09	203.12	19.36	50.00	84.44	83.33	40.00	72.10	65.98
TakeAD [27]	RA-L 26	71.39	40.83	193.30	22.89	30.77	35.56	56.67	50.00	42.02	43.00
<i>Vision Language Action Methods</i>											
DriveMOE [47]	arXiv 25	74.22	48.64	175.96	15.31	34.67	40.00	65.45	40.00	59.44	47.91
ORION [11]	ICCV 25	77.74	54.62	151.48	17.38	25.00	71.11	78.33	30.00	69.15	54.72
MindDrive [12]	arXiv 26	78.04	55.09	-	-	32.89	75.56	68.33	50.00	57.89	56.94
AutoVLA [54]	NeurIPS 25	78.84	57.73	146.93	39.33	-	-	-	-	-	-
RecogDrive [24]	ICLR 26	71.36	45.45	138.18	17.45	29.73	20.00	69.09	20.00	71.34	42.03
SimLingo* [32]	CVPR 25	84.79	64.84	248.79	28.61	51.90	53.33	85.00	50.00	78.42	63.73
TakeVLA (Ours)	-	89.72	73.73	249.01	30.27	63.64	64.44	91.67	50.00	85.48	71.05
<i>Privileged Methods</i>											
Think2Drive [22]	ECCV 24	91.85	85.41	269.14	25.97	81.27	83.92	90.24	90.00	87.67	86.26
PDM-Lite* [38]	CVPRW 24	96.25	83.49	213.47	22.33	82.05	91.11	81.67	80.00	70.97	81.16

* Reproduced using official implementation.

Implementation Details. For pre-training, we strictly follow the official SimLingo [32] setup, training for 14 epochs with a total batch size of 64. For post-training, SFT uses the same batch size and runs for 8 epochs. RFT updates only the LLM while freezing other components to ensure training stability. We employ GRPO for policy optimization with a group size $G = 8$, KL weight $\lambda = 0.1$, and a sampling temperature of 1.0, training for 1 epoch with a total batch size of 32. The discount factor $\gamma = 0.9$. Both SFT and RFT use a learning rate of $3e-6$ with a cosine annealing schedule. All experiments are conducted on $8 \times$ NVIDIA H20 GPUs. The LLM is updated via LoRA [15], maintaining consistent configurations across both pre-training and post-training stages.

5.2 Main Results

SoTA performance on Bench2Drive. Tab. 1 presents closed-loop driving performance of state-of-the-art (SoTA) methods on the B2D leaderboard. The left part shows overall driving metrics. Among all end-to-end methods, TakeVLA achieves the highest driving score and success rate, substantially outperforming our baseline method SimLingo [32] by 4.93 points and 8.89% , respectively. B2D further provides multi-ability evaluation, categorizing all test routes into different ability types, with each ability score defined as the success rate across all routes of that type. As shown in the right part of Tab. 1, TakeVLA leads in the multi-ability mean score and nearly dominates all individual abilities. These results demonstrate the effectiveness of our post-training framework in achieving superior closed-loop performance for driving VLA models.

Improved Performance without Rule-based Post-process. Existing methods often rely on rule-based post-processing to boost performance met-

Table 2: Closed-loop performance without rule-based post-process.

Methods	Closed-loop Metric		
	DS \uparrow	SR (%) \uparrow	TR (%) \downarrow
SimLingo \dagger	79.19	55.50	12.39
TakeVLA (Ours) \dagger	86.44	68.20	9.22

 \dagger Without creep.

rics [39, 41]. SimLingo uses the creep technique [7] to force forward motion when the ego-vehicle remains stationary for an extended period. While creep helps escape stuck states in practice, it introduces potential safety risks and highlights limitations in the model’s intrinsic stop-go reasoning. We address this by applying post-training with restart-triggered takeover data and language label enhancement. As shown in Tab. 2, the Timeout Rate (TR) metric measures the proportion of routes that fail due to timeout. Without any creep post-processing, TakeVLA maintains SoTA performance while achieving a noticeably higher driving score (+7.25) and lower timeout rate (-3.17%) compared to SimLingo. These results show that our post-training framework delivers strong closed-loop performance without rule-based post-processing, enhancing intrinsic stop-go reasoning.

5.3 Ablation Studies

In this section, we conduct ablation studies to evaluate the contribution of each component and key hyperparameter in TakeVLA. All reported results, except for multi-round training, are obtained from **the first round** of post-training. To directly quantify the model’s proactive collision avoidance capability and safety margin, we introduce the average Time-to-Collision (TTC) metric, defined as:

$$\text{TTC} = \frac{\sum_{i=1}^{N_a} \text{TTC}_i}{N_a}, \text{TTC}_i = \frac{d_i}{v_{\text{rel},i}}, \quad (4)$$

where N_a is the total number of traffic participants that the ego encounters during evaluation. The variable $v_{\text{rel},i}$ denotes the relative velocity between the ego and the i -th participant, while d_i represents their corresponding relative distance. In practice, TTC_i is computed only for participants located ahead of the ego, with positive relative velocity, and within 100m.

Table 3: Ablation study on post-training techniques of TakeVLA.

ID	Post-training Techniques				Closed-loop Metric \uparrow		
	Takeover Data	Label Enhancement	Pre-takeover	Scenario Dreaming	DS	SR (%)	TTC (s)
1	\times	\times	\times	\times	84.79	64.84	7.23
2	\checkmark	\times	\times	\times	86.22	68.52	7.56
3	\checkmark	\checkmark	\times	\times	86.73	68.04	7.53
4	\checkmark	\checkmark	\checkmark	\times	87.25	68.35	7.99
5	\checkmark	\checkmark	\checkmark	\checkmark	87.79	68.81	8.16

Ablation on Post-training Techniques. Tab. 3 presents closed-loop performance under different combinations of post-training techniques. The baseline model (ID 1), without any post-training, achieves a driving score of 84.79, a success rate of 64.84%, and an average TTC of 7.23 seconds. Incorporating takeover data alone (ID 2) significantly improves the driving score by 1.43 points and TTC by 0.33 seconds, demonstrating that takeover data effectively mitigates distribution shift. Adding language label enhancement (ID 3) further boosts the driving score, confirming the benefit of refined language labels for better decision-making. Introducing pre-takeover supervision (ID 4) noticeably increases TTC by 0.43 seconds, validating its role in enlarging safety margins. Finally, enabling Scenario Dreaming (ID 5) yields the highest performance, with a driving score of 87.79 and a TTC of 8.16 seconds, showing that active exploration further optimizes the model in safety-critical scenarios.

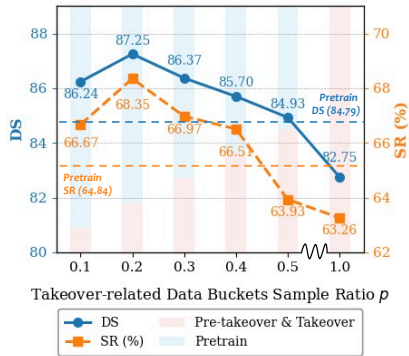


Fig. 5: Impact of sampling ratio during SFT. The colored bar visualizes the sampling ratio between pre-training and takeover-related buckets.

Ablation on Sample Ratio. During SFT, we follow the bucket sampling strategy and assign sampling probability p to buckets derived from takeover-related datasets $\mathcal{D}_{takeover}$ and $\mathcal{D}_{pre-takeover}$, and $1 - p$ to buckets from the pre-training dataset $\mathcal{D}_{pretrain}$. Fig. 5 shows closed-loop performance as p varies from 0.1 to 1.0, with the pre-training baseline as reference. Performance peaks at $p = 0.2$, achieving the highest driving score of 87.25 and a success rate of 68.35%, significantly outperforming the baseline. As p increases beyond 0.2, both driving score and success rate gradually decline, reaching the lowest values at $p = 1.0$. This trend indicates that a moderate proportion of takeover samples effectively balances the learning of corrective behaviors while maintaining pre-training capabilities. Consequently, we set $p = 0.2$ as the default to achieve the best trade-off.

Ablation on GRPO Group Size and Reward Design. As shown in Tab. 4, with both distance and collision terms enabled, performance steadily improves as the group size G increases from 2 to 8 (IDs 1–4). The best overall results are achieved at $G = 8$, indicating that a larger group size yields more stable group-relative advantage estimation and better policy optimization. Ab-

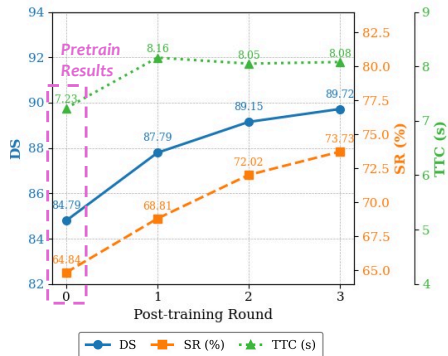


Fig. 6: Multi-round post-training performance. TakeVLA shows progressive performance gains in core driving metrics across rounds.

Table 4: Effects of group size and reward design for GRPO training.

ID	Group	Reward terms		Closed-loop Metric \uparrow		
	size G	Distance	Collision	DS	SR (%)	TTC (s)
1	2	✓	✓	86.88	68.35	8.05
2	4	✓	✓	87.33	67.28	8.01
3	6	✓	✓	87.48	69.41	8.19
4	8	✓	✓	87.79	68.81	8.16
5	8	✓	✗	87.22	68.81	7.54
6	8	✗	✓	87.28	68.69	7.88

lating reward terms (IDs 5 and 6) reveals their complementary roles, as removing either term alone degrades performance, particularly in safety margins. Specifically, removing the collision reward causes a clear drop in TTC, highlighting the importance of explicit collision avoidance optimization. Removing the distance term leads to a milder TTC decline, indicating that collision rewards alone fail to provide comprehensive guidance. The distance term implicitly encodes certain hard-to-model reward signals from expert behaviors, thereby steering optimization toward better alignment with the demonstration policy.

Ablation on the Number of Post-training Rounds. Fig. 6 illustrates the progressive performance gains of TakeVLA across multiple post-training rounds. Both driving score and success rate exhibit consistent improvements with each additional round, confirming that iterative post-training refines model behavior and enhances closed-loop performance. TTC reaches near-peak values after the first round and remains stable thereafter, with only minor fluctuations. By the third round, TakeVLA achieves substantial improvements over the pre-trained baseline, increasing driving score by 4.93, success rate by 8.89%, and TTC by 0.85 (a relative increase of 11.76%). The diminishing marginal gains, particularly TTC saturation after the first round, likely stem from information asymmetry between the expert and the VLA model [28]. The expert has access to comprehensive contextual information beyond the front-view camera input available to the VLA, which limits the model’s ability to further close the performance gap in later rounds. Future work will investigate expanded perceptual inputs and techniques from [28] to mitigate this asymmetry and enable more effective continual learning.

5.4 Qualitative Results

Fig. 7 provides a qualitative comparison of SimLingo and TakeVLA along a continuous driving route, which requires the ego-vehicle to bypass a construction site while yielding to continuous left-lane traffic. The selected frames in sequence illustrate key moments of the route. SimLingo generates brief language outputs that fail to anticipate lane-change risks, resulting in unsafe timing (*e.g.*, initiating lane change without sufficient gap) and subsequent collisions, as well as delayed braking in car-following scenarios, causing rear-end collisions. In contrast, TakeVLA produces richer, more context-aware language outputs that explicitly consider upcoming hazards and gaps, leading to successful collision avoidance

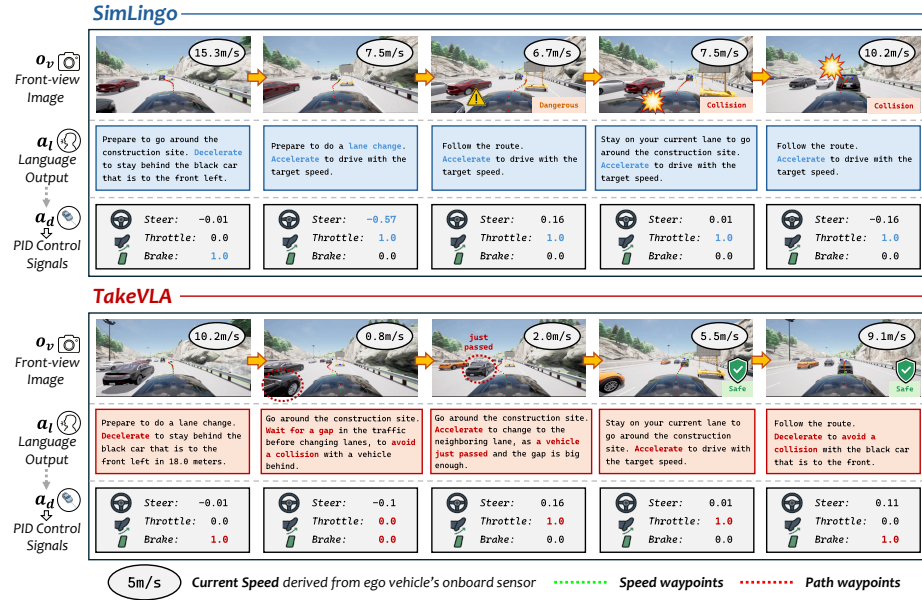


Fig. 7: Qualitative visualization of SimLingo and TakeVLA. Each column shows a selected frame in temporal order. Driving action a_d is drawn on the front-view image in the form of speed and path waypoints. The PID control signals are generated from a_d . We omit the language input o_l for brevity. SimLingo generates insufficient language outputs, leading to unsafe lane changes and rear-end collisions. TakeVLA generates more anticipatory and context-aware language outputs, enabling safer gap selection, timely acceleration, and proactive deceleration to avoid collisions.

during lane-changing and car-following while maintaining smooth driving. These examples illustrate how our proposed post-training framework enables safer and more reliable driving behavior.

6 Conclusion

In this paper, we presented TakeVLA, a novel post-training framework that effectively leverages expert takeover data to enhance pre-trained Vision-Language-Action (VLA) models for end-to-end autonomous driving. By introducing pre-takeover language supervision tailored to takeover trigger conditions, TakeVLA enables proactive hazard anticipation through improved language output quality. Complementing this, our Scenario Dreaming mechanism performs reinforcement fine-tuning in reconstructed takeover scenarios, encouraging active exploration to achieve optimal policies beyond passive preference imitation. Extensive closed-loop evaluation on the Bench2Drive benchmark demonstrates that TakeVLA achieves state-of-the-art performance while significantly improving safety mar-

gins. We believe TakeVLA represents a practical step toward building safer, more reliable, and interpretable VLA systems for autonomous driving.

References

1. Black, K., Brown, N., Driess, D., Esmail, A., Equi, M.R., Finn, C., Fusai, N., Groom, L., Hausman, K., Ichter, B., Jakubczak, S., Jones, T., Ke, L., Levine, S., Li-Bell, A., Mothukuri, M., Nair, S., Pertsch, K., Shi, L.X., Smith, L., Tanner, J., Vuong, Q., Walling, A., Wang, H., Zhilinsky, U.: $\pi 0$: A Vision-Language-Action Flow Model for General Robot Control. In: Proceedings of Robotics: Science and Systems. Los Angeles, CA, USA (June 2025). <https://doi.org/10.15607/RSS.2025.XXI.010>
2. Cai, H., Peng, Z., Zhou, B.: Predictive preference learning from human interventions. arXiv preprint arXiv:2510.01545 (2025)
3. Cao, W., Hallgarten, M., Li, T., Dauner, D., Gu, X., Wang, C., Miron, Y., Aiello, M., Li, H., Gilitschenski, I., Ivanovic, B., Pavone, M., Geiger, A., Chitta, K.: Pseudo-simulation for autonomous driving. In: Conference on Robot Learning (CoRL) (2025)
4. Chen, L., Wu, P., Chitta, K., Jaeger, B., Geiger, A., Li, H.: End-to-end autonomous driving: Challenges and frontiers. *IEEE Transactions on Pattern Analysis and Machine Intelligence* **46**(12), 10164–10183 (2024)
5. Chen, S., Jiang, B., Gao, H., Liao, B., Xu, Q., Zhang, Q., Huang, C., Liu, W., Wang, X.: Vadv2: End-to-end vectorized autonomous driving via probabilistic planning. arXiv preprint arXiv:2402.13243 (2024)
6. Chen, Z., Wu, J., Wang, W., Su, W., Chen, G., Xing, S., Zhong, M., Zhang, Q., Zhu, X., Lu, L., et al.: Internvl: Scaling up vision foundation models and aligning for generic visual-linguistic tasks. In: Proceedings of the IEEE/CVF conference on computer vision and pattern recognition. pp. 24185–24198 (2024)
7. Chitta, K., Prakash, A., Jaeger, B., Yu, Z., Renz, K., Geiger, A.: Transfuser: Imitation with transformer-based sensor fusion for autonomous driving. *IEEE Transactions on Pattern Analysis and Machine Intelligence* **45**(11), 12878–12895 (2023). <https://doi.org/10.1109/TPAMI.2022.3200245>
8. Dauner, D., Hallgarten, M., Li, T., Weng, X., Huang, Z., Yang, Z., Li, H., Gilitschenski, I., Ivanovic, B., Pavone, M., Geiger, A., Chitta, K.: Navsim: Data-driven non-reactive autonomous vehicle simulation and benchmarking. In: Advances in Neural Information Processing Systems (NeurIPS) (2024)
9. Dosovitskiy, A., Ros, G., Codevilla, F., Lopez, A., Koltun, V.: Carla: An open urban driving simulator. In: Conference on robot learning. pp. 1–16. PMLR (2017)
10. Fang, S., Cui, Y., Liang, H., Lv, C., Hang, P., Sun, J.: Corevla: A dual-stage end-to-end autonomous driving framework for long-tail scenarios via collect-and-refine. arXiv preprint arXiv:2509.15968 (2025)
11. Fu, H., Zhang, D., Zhao, Z., Cui, J., Liang, D., Zhang, C., Zhang, D., Xie, H., Wang, B., Bai, X.: Orion: A holistic end-to-end autonomous driving framework by vision-language instructed action generation. In: Proceedings of the IEEE/CVF International Conference on Computer Vision. pp. 24823–24834 (2025)
12. Fu, H., Zhang, D., Zhao, Z., Cui, J., Xie, H., Wang, B., Chen, G., Liang, D., Bai, X.: Minddrive: A vision-language-action model for autonomous driving via online reinforcement learning. arXiv preprint arXiv:2512.13636 (2025)

13. Gao, Y., Liu, Y., Zhang, Q., Wang, Y., Zhao, D., Ding, D., Pang, Z., Zhang, Y.: Comparison of control methods based on imitation learning for autonomous driving. In: 2019 Tenth International Conference on Intelligent Control and Information Processing (ICICIP). pp. 274–281 (2019). <https://doi.org/10.1109/ICICIP47338.2019.9012185>
14. Gao, Y., Zhang, Q., Ding, D.W., Zhao, D.: Dream to drive with predictive individual world model. *IEEE Transactions on Intelligent Vehicles* **9**(12), 8224–8238 (2024). <https://doi.org/10.1109/TIV.2024.3408830>
15. Hu, E.J., Shen, Y., Wallis, P., Allen-Zhu, Z., Li, Y., Wang, S., Wang, L., Chen, W.: Lora: Low-rank adaptation of large language models (2021), <https://arxiv.org/abs/2106.09685>
16. Hu, Y., Yang, J., Chen, L., Li, K., Sima, C., Zhu, X., Chai, S., Du, S., Lin, T., Wang, W., et al.: Planning-oriented autonomous driving. In: Proceedings of the IEEE/CVF conference on computer vision and pattern recognition. pp. 17853–17862 (2023)
17. Jia, X., Yang, Z., Li, Q., Zhang, Z., Yan, J.: Bench2drive: Towards multi-ability benchmarking of closed-loop end-to-end autonomous driving. *Advances in Neural Information Processing Systems* **37**, 819–844 (2024)
18. Jia, X., You, J., Zhang, Z., Yan, J.: Drivetransformer: Unified transformer for scalable end-to-end autonomous driving. *arXiv preprint arXiv:2503.07656* (2025)
19. Jiang, B., Chen, S., Xu, Q., Liao, B., Chen, J., Zhou, H., Zhang, Q., Liu, W., Huang, C., Wang, X.: Vad: Vectorized scene representation for efficient autonomous driving. In: Proceedings of the IEEE/CVF International Conference on Computer Vision. pp. 8340–8350 (2023)
20. Jiang, B., Chen, S., Zhang, Q., Liu, W., Wang, X.: Alphadrive: Unleashing the power of vlms in autonomous driving via reinforcement learning and reasoning. *arXiv preprint arXiv:2503.07608* (2025)
21. Kim, M.J., Pertsch, K., Karamcheti, S., Xiao, T., Balakrishna, A., Nair, S., Rafailov, R., Foster, E.P., Sanketi, P.R., Vuong, Q., Kollar, T., Burchfiel, B., Tedrake, R., Sadigh, D., Levine, S., Liang, P., Finn, C.: OpenVLA: An open-source vision-language-action model. In: 8th Annual Conference on Robot Learning (2024), <https://openreview.net/forum?id=ZMnD6QZAE6>
22. Li, Q., Jia, X., Wang, S., Yan, J.: Think2drive: Efficient reinforcement learning by thinking with latent world model for autonomous driving (in carla-v2). In: European conference on computer vision. pp. 142–158. Springer (2024)
23. Li, Y., Fan, L., He, J., Wang, Y., Chen, Y., Zhang, Z., Tan, T.: Enhancing end-to-end autonomous driving with latent world model. *arXiv preprint arXiv:2406.08481* (2024)
24. Li, Y., Xiong, K., Guo, X., Li, F., Yan, S., Xu, G., Zhou, L., Chen, L., Sun, H., Wang, B., et al.: Recogdrive: A reinforced cognitive framework for end-to-end autonomous driving. *arXiv preprint arXiv:2506.08052* (2025)
25. Li, Z., Wang, S., Lan, S., Yu, Z., Wu, Z., Alvarez, J.M.: Hydra-next: Robust closed-loop driving with open-loop training. In: Proceedings of the IEEE/CVF International Conference on Computer Vision. pp. 27305–27314 (2025)
26. Liao, B., Chen, S., Yin, H., Jiang, B., Wang, C., Yan, S., Zhang, X., Li, X., Zhang, Y., Zhang, Q., et al.: Diffusiondrive: Truncated diffusion model for end-to-end autonomous driving. In: Proceedings of the Computer Vision and Pattern Recognition Conference. pp. 12037–12047 (2025)
27. Liu, D., Gao, Y., Qian, D., Zhang, Q., Ye, X., Han, J., Zheng, Y., Liu, X., Xia, Z., Ding, D., et al.: Takead: Preference-based post-optimization for end-to-end

- autonomous driving with expert takeover data. *IEEE Robotics and Automation Letters* **11**(2), 1738–1745 (2025)
28. Nguyen, L., Fauth, M., Jaeger, B., Dauner, D., Igl, M., Geiger, A., Chitta, K.: Lead: Minimizing learner-expert asymmetry in end-to-end driving. In: *Conference on Computer Vision and Pattern Recognition (CVPR)* (2026)
 29. Ouyang, L., Wu, J., Jiang, X., Almeida, D., Wainwright, C., Mishkin, P., Zhang, C., Agarwal, S., Slama, K., Ray, A., et al.: Training language models to follow instructions with human feedback. *Advances in neural information processing systems* **35**, 27730–27744 (2022)
 30. Peng, Z., Luo, W., Lu, Y., Shen, T., Gulino, C., Seff, A., Fu, J.: Improving agent behaviors with rl fine-tuning for autonomous driving. In: *European Conference on Computer Vision*. pp. 165–181. Springer (2024)
 31. Rafailov, R., Sharma, A., Mitchell, E., Ermon, S., Manning, C.D., Finn, C.: Direct preference optimization: Your language model is secretly a reward model (2024), <https://arxiv.org/abs/2305.18290>
 32. Renz, K., Chen, L., Arani, E., Sinavski, O.: Simlingo: Vision-only closed-loop autonomous driving with language-action alignment. In: *Proceedings of the Computer Vision and Pattern Recognition Conference*. pp. 11993–12003 (2025)
 33. Ross, S., Gordon, G., Bagnell, D.: A reduction of imitation learning and structured prediction to no-regret online learning. In: *Proceedings of the fourteenth international conference on artificial intelligence and statistics*. pp. 627–635. *JMLR Workshop and Conference Proceedings* (2011)
 34. Rowe, L., de Schaetzen, R., Girgis, R., Pal, C., Paull, L.: Poutine: Vision-language-trajectory pre-training and reinforcement learning post-training enable robust end-to-end autonomous driving. *arXiv preprint arXiv:2506.11234* (2025)
 35. Shao, H., Hu, Y., Wang, L., Song, G., Waslander, S.L., Liu, Y., Li, H.: Lmdrive: Closed-loop end-to-end driving with large language models. In: *Proceedings of the IEEE/CVF conference on computer vision and pattern recognition*. pp. 15120–15130 (2024)
 36. Shao, Z., Wang, P., Zhu, Q., Xu, R., Song, J., Bi, X., Zhang, H., Zhang, M., Li, Y., Wu, Y., et al.: Deepseekmath: Pushing the limits of mathematical reasoning in open language models. *arXiv preprint arXiv:2402.03300* (2024)
 37. Shi, L.X., Hu, Z., Zhao, T.Z., Sharma, A., Pertsch, K., Luo, J., Levine, S., Finn, C.: Yell At Your Robot: Improving On-the-Fly from Language Corrections. In: *Proceedings of Robotics: Science and Systems*. Delft, Netherlands (July 2024). <https://doi.org/10.15607/RSS.2024.XX.025>
 38. Sima, C., Renz, K., Chitta, K., Chen, L., Zhang, H., Xie, C., Beißwenger, J., Luo, P., Geiger, A., Li, H.: Drivelm: Driving with graph visual question answering. In: *European conference on computer vision*. pp. 256–274. Springer (2024)
 39. Sun, W., Lin, X., Shi, Y., Zhang, C., Wu, H., Zheng, S.: Sparsedrive: End-to-end autonomous driving via sparse scene representation. In: *2025 IEEE International Conference on Robotics and Automation (ICRA)*. pp. 8795–8801. IEEE (2025)
 40. Sutton, R.S., Barto, A.G., et al.: *Reinforcement learning: An introduction*, vol. 1. MIT press Cambridge (1998)
 41. Tang, Y., Xu, Z., Meng, Z., Cheng, E.: Hip-ad: Hierarchical and multi-granularity planning with deformable attention for autonomous driving in a single decoder. In: *Proceedings of the IEEE/CVF International Conference on Computer Vision*. pp. 25605–25615 (2025)
 42. Tian, H., Li, T., Liu, H., Yang, J., Qiu, Y., Li, G., Wang, J., Gao, Y., Zhang, Z., Wang, L., Ye, H., Tan, T., Chen, L., Li, H.: Simscale: Learning to drive via real-world simulation at scale (2025), <https://arxiv.org/abs/2511.23369>

43. Wang, J., Liu, X., Zheng, Y., Xing, Z., Li, P., Li, G., Ma, K., Chen, G., Ye, H., Xia, Z., Chen, L., Zhang, Q.: Meanfuser: Fast one-step multi-modal trajectory generation and adaptive reconstruction via meanflow for end-to-end autonomous driving (2026), <https://arxiv.org/abs/2602.20060>
44. Wang, Y., Luo, W., Bai, J., Cao, Y., Che, T., Chen, K., Chen, Y., Diamond, J., Ding, Y., Ding, W., et al.: Alpamayo-r1: Bridging reasoning and action prediction for generalizable autonomous driving in the long tail. arXiv preprint arXiv:2511.00088 (2025)
45. Yang, A., Yang, B., Hui, B., Zheng, B., Yu, B., Zhou, C., Li, C., Li, C., Liu, D., Huang, F., Dong, G., Wei, H., Lin, H., Tang, J., Wang, J., Yang, J., Tu, J., Zhang, J., Ma, J., Yang, J., Xu, J., Zhou, J., Bai, J., He, J., Lin, J., Dang, K., Lu, K., Chen, K., Yang, K., Li, M., Xue, M., Ni, N., Zhang, P., Wang, P., Peng, R., Men, R., Gao, R., Lin, R., Wang, S., Bai, S., Tan, S., Zhu, T., Li, T., Liu, T., Ge, W., Deng, X., Zhou, X., Ren, X., Zhang, X., Wei, X., Ren, X., Liu, X., Fan, Y., Yao, Y., Zhang, Y., Wan, Y., Chu, Y., Liu, Y., Cui, Z., Zhang, Z., Guo, Z., Fan, Z.: Qwen2 technical report (2024), <https://arxiv.org/abs/2407.10671>
46. Yang, P., Lu, B., Xia, Z., Han, C., Gao, Y., Zhang, T., Zhan, K., Lang, X., Zheng, Y., Zhang, Q.: Worldrft: Latent world model planning with reinforcement fine-tuning for autonomous driving. arXiv preprint arXiv:2512.19133 (2025)
47. Yang, Z., Chai, Y., Jia, X., Li, Q., Shao, Y., Zhu, X., Su, H., Yan, J.: Drivemoe: Mixture-of-experts for vision-language-action model in end-to-end autonomous driving. arXiv preprint arXiv:2505.16278 (2025)
48. Yang, Z., Jia, X., Li, Q., Yang, X., Yao, M., Yan, J.: Raw2drive: Reinforcement learning with aligned world models for end-to-end autonomous driving (in carla v2). arXiv preprint arXiv:2505.16394 (2025)
49. Zeng, S., Chang, X., Xie, M., Liu, X., Bai, Y., Pan, Z., Xu, M., Wei, X., Guo, N.: Futuresightdrive: Thinking visually with spatio-temporal cot for autonomous driving. arXiv preprint arXiv:2505.17685 (2025)
50. Zhang, Q., Gao, Y., Zhang, Y., Guo, Y., Ding, D., Wang, Y., Sun, P., Zhao, D.: Trajgen: Generating realistic and diverse trajectories with reactive and feasible agent behaviors for autonomous driving. *IEEE Transactions on Intelligent Transportation Systems* **23**(12), 24474–24487 (2022). <https://doi.org/10.1109/TITS.2022.3202185>
51. Zheng, W., Song, R., Guo, X., Zhang, C., Chen, L.: Genad: Generative end-to-end autonomous driving. In: *European Conference on Computer Vision*. pp. 87–104. Springer (2024)
52. Zheng, Y., Xing, Z., Zhang, Q., Jin, B., Li, P., Zheng, Y., Xia, Z., Chen, Y., Zhao, D.: Planagent: A multi-modal large language agent for closed-loop vehicle motion planning. *IEEE Transactions on Cognitive and Developmental Systems* pp. 1–14 (2026). <https://doi.org/10.1109/TCDS.2026.3664120>
53. Zheng, Y., Yang, P., Xing, Z., Zhang, Q., Zheng, Y., Gao, Y., Li, P., Zhang, T., Xia, Z., Jia, P., et al.: World4drive: End-to-end autonomous driving via intention-aware physical latent world model. In: *Proceedings of the IEEE/CVF International Conference on Computer Vision*. pp. 28632–28642 (2025)
54. Zhou, Z., Cai, T., Zhao, S.Z., Zhang, Y., Huang, Z., Zhou, B., Ma, J.: Autovla: A vision-language-action model for end-to-end autonomous driving with adaptive reasoning and reinforcement fine-tuning. arXiv preprint arXiv:2506.13757 (2025)
55. Zimmerlin, J., Beißwenger, J., Jaeger, B., Geiger, A., Chitta, K.: Hidden biases of end-to-end driving datasets. arXiv preprint arXiv:2412.09602 (2024)